Research Article

Effect of Milling on DSC Thermogram of Excipient Adipic Acid

Wai Kiong Ng,[1,3] Jin Wang Kwek,[1] Aaron Yuen,[1] Chin Lee Tan,[1] and Reginald Tan[1,2,3]

Abstract. The purpose of this research was to investigate why and how mechanical milling results in an unexpected shift in differential scanning calorimetry (DSC) measured fusion enthalpy ($\Delta_{\text{fus}}H$) and melting point (T_{m}) of adipic acid, a pharmaceutical excipient. Hyper differential scanning calorimetry (hyper-DSC) was used to characterize adipic acid before and after ball-milling. An experimental study was conducted to evaluate previous postulations such as electrostatic charging using the Faraday cage method, crystallinity loss using powder X-ray diffraction (PXRD), thermal annealing using DSC, impurities removal using thermal gravimetric analysis (TGA) and Karl Fischer titration. DSC thermograms showed that after milling, the values of $\Delta_{\text{fus}}H$ and T_{m} were increased by approximately 9% and 5 K, respectively. Previous suggestions of increased electrostatic attraction, change in particle size distribution, and thermal annealing during measurements did not explain the differences. Instead, theoretical analysis and experimental findings suggested that the residual solvent (water) plays a key role. Water entrapped as inclusions inside adipic acid during solution crystallization was partially evaporated by localized heating at the cleaved surfaces during milling. The correlation between the removal of water and melting properties measured was shown via drying and crystallization experiments. These findings show that milling can reduce residual solvent content and causes a shift in DSC results.

KEY WORDS: DSC; fusion enthalpy; impurity; melting temperature; milling.

INTRODUCTION

Milling, also known as comminution or grinding, is typically regarded as a particle size reduction process across many industries, including the manufacturing of pharmaceuticals and fine chemicals. In secondary pharmaceutical processing, milling is often used to increase the specific surface area of poorly water-soluble drugs, so as to improve their dissolution properties and bioavailability (1). Comminution is also used to improve the uniformity of particle size leading to better mixing properties critical in solid dosage form production (2,3). However, besides reducing the particle size, the milling process is often accompanied by other unintended effects such as changes in morphology (4), crystallinity (5), polymorphism (6), glass transition temperatures (7), chemical stability (8), melting properties (9,10), as well as particle size shifts (11) and specific surface area increase (12) during subsequent post-milling storage. Though undesired, such secondary effects are not well reported and often hard to predict. Although the melting behavior is widely studied in materials research, Vitez and Newman (13) mentioned that

the impact on thermal characterization due to such processing-induced changes is not fully understood. Therefore, the aim of this paper is to characterize and provide more understanding to the change in melting properties of adipic acid, an excipient, due to the milling process.

Previous reports (9,14) showed that milling can either cause an increase or reduction in the enthalpy of fusion ($\Delta_{\text{fus}}H$) and melting temperature (T_{m}). Although a few plausible reasons have been suggested to account for this phenomenon, there are few experimental studies to account for it. Van Dooren and Müller (15–19) reported higher values of $\Delta_{\text{fus}}H$ and onset T_{m} of adipic acid ground in a mortar with a pestle when compared to untreated adipic acid. They proposed that the enthalpy increase may be due to the breaking of electrostatic forces between milled aggregates, which required energy that is added to the melting endotherm. Milling is known to cause triboelectrification of particles and induce electrostatic charges ranging from 0.1×10^{-9} C/g to 100×10^{-9} C/g as given in the British Standard 5958 (20). Electrostatic charging could have resulted from the collision and sliding between particle–particle and particle–wall. Besides electrostatic charges, it was also reported that coarse adipic acid particles with a narrower size distribution possessed lower values of onset T_{m} and $\Delta_{\text{fus}}H$ than those from a complete size spectrum. It was attributed to greater thermal resistance in the coarse particle sample than in the sample containing some fine particles. Coarse particles in contact with the "hot" side of the DSC heating pan may melt before releasing energy to other particles, resulting in lower onset T_{m} and $\Delta_{\text{fus}}H$. As grinding is known to impart

[1] Institute of Chemical and Engineering Sciences, Agency for Science, Technology and Research (A*STAR), 1 Pesek Road, Jurong Island, Singapore, Singapore 627833.
[2] Department of Chemical and Biomolecular Engineering, National University of Singapore, 4 Engineering Drive 4, Singapore, Singapore 117576.
[3] To whom correspondence should be addressed. (e-mail: ng_wai_kiong@ices.a-star.edu.sg; reginald@ices.a-star.edu.sg)

structural disorders in crystalline structure of solids, it was discussed whether a reduction in the degree of crystallinity could increase T_m and $\Delta_{fus}H$. However, since less energy was required to destroy (melt) structures of lower crystal perfection, the observed increase in T_m and $\Delta_{fus}H$ of milled adipic acid could not be accounted for. Discussions on reduced crystallinity in increasing the $\Delta_{fus}H$ of milled materials were more recently revived by Chikhalia and co-workers [14]. Similarly, an increase in $\Delta_{fus}H$ after milling β-succinic acid, a dicarboxylic acid structurally similar to adipic acid, was measured by DSC. It was suggested that milling reduced the crystallinity of succinic acid particles. During DSC analysis, the occurrence of thermal annealing of the amorphous content led to the differences in $\Delta_{fus}H$ measured. It was shown that when thermal analysis was repeated at high heating rates of 50°C/min, the difference in $\Delta_{fus}H$ values between untreated and milled succinic acid became less apparent as there was insufficient time for thermal annealing to take place.

Révész [9] ball-milled aluminum (Al) powders for different milling times ranging from 45 min to 32 days. Contrary to adipic acid, the T_m of aluminum powders was reduced upon milling, which further decreases with increasing milling time. It was shown that the microstructure of nano-crystalline Al powders underwent a significant change during ball-milling. The melting point depression was found to be proportional to inverse grain size. Similarly, mechanical milling or thermal annealing at 150°C was shown to decrease the $\Delta_{fus}H$ and T_m of dipyridamole, a widely used anti-aggregating agent mostly employed to prevent repeated heart attacks. Fourier-transform infrared photoacoustic spectro-scopic (FTIR/PAS) data suggested that the transformation of intramolecular H-bonds into intermolecular H-bonds of the cyclic systems was responsible for the decrease in melting properties [10]. Feng *et al.* [21] also reported that $\Delta_{fus}H$ and T_m of cryomilled griseofulvin, an anti-fungal agent, both decrease with longer milling times, which was explained by weakened intermolecular interactions that require less energy to break up all the bonds among molecules. Vitez and Newman [13] reported that the processing method may play an important role in the onset T_m of a material. The re-crystallization processes, including the solvent and mechanical systems utilized to manufacture the material, may greatly affect the crystallinity. This would directly influence the amorphous content in the presumably high crystalline material through the production of an "impurity" which would lower the onset T_m of the material. Law [22] reported a correlation between water content entrapped in crystallized adipic acid and $\Delta_{fus}H$. However, it was not mentioned whether milling could alter the water content inside adipic acid and in turn, influence $\Delta_{fus}H$. This work examines the various postulated reasons behind milling-induced changes in the melting properties such as electrostatic charging, particle size effect, crystallinity, amorphization, and water content.

Adipic acid was chosen as a model compound to provide a comparison to earlier reports. It is a pharmaceutical excipient commonly used as an effervescent or a lubricating material in tablets formulation. Adipic acid also has an advantage of having no reported polymorph and stoichio-metric hydrates/solvates, which may have additional effects on the melting properties after milling [23]. Thermal proper-ties $\Delta_{fus}H$ and T_m are studied using DSC because they are important solid-state characteristics of pharmaceutical com-pounds. DSC analysis spans across the entire range of pharmaceutical research from preformulation screening, lab-oratory-scale and pilot process development to quality control during commercial manufacturing and is recommen-ded as one of the characterization techniques in the "Gold Sheet" [23,24]. Accurate values of $\Delta_{fus}H$ and T_m are needed to determine product purity, used in theoretical predictions of aqueous solubility of new pharmaceutical compounds [25] as well as input parameters for the design of melt crystallizers and hot melt extruders.

MATERIALS AND METHODS

Materials

Adipic acid (Sigma-Aldrich) was crystallized in de-ionized (DI) water using the batch-cooling method described by Keel *et al.* [26] About 28 g of adipic acid were dissolved in 400 ml of DI water at 25°C inside a 500-ml jacketed batch crystallizer. The solution was heated to 60°C to ensure complete dissolution before being cooled at 1°C/min to room temperature. The crystals obtained were vacuum-filtered and dried for 24 h in an oven at 55°C. Samples were kept inside a dessicator maintained below 20% relative humidity (RH) using phosphorus pentoxide (P_2O_5). Crystallized adipic acid was milled using a planetary ball mill (Fritsch Pulverisette 5, Germany). Milling was carried out with stainless steel balls (10 mm diameter) at ball to sample mass ratio of 50:1 and at 400 rpm for 30 min. Crystallized and milled adipic acid samples were sieved using an analytical sieve shaker (Retsch AS200 Control, Germany) to obtain a consistent size fraction for subsequent analyses. The sieve shaker was operated at an amplitude of 2.5 and pulse mode of 10 s for a duration of 10 min. Sieves with mesh width of 1,000, 710, 500, 250, 106, and 38 μm were used. Crystallized and milled adipic acid of size fraction between 250 and 500 μm were selected for subsequent analyses.

To prepare adipic acid with different water contents, approximately 100 mg of crystallized adipic acid was divided into 5 ml glass vials and kept inside an oven set at 110°C. Samples were collected every 2 h, capped tightly and then kept in a dessicator at low humidity conditions prior to analysis. In addition, to eliminate any possible effects of heating on the samples, the same batch-cooling crystallization method was used to prepare adipic acid with varying water contents by using different cooling rates at 0.67, 0.33, and 0.033°C/min.

Analytical Methods

The surface morphology of the crystallized and milled adipic acid samples was imaged using the field emission scanning electron microscope (SEM, JSM-6700F, JEOL, Japan). Electrostatic charge measurements ($n=3$) were car-ried out inside a humidity chamber kept below 20% RH with a Faraday cage (TR8031, Advantest, Japan) connected to an electrometer (Keithley 6517A, USA). The water content of adipic acid was determined using a Karl Fisher titrator (Metrohm 831 KF Coulometer, Switzerland; $n=3$). For each

measurement, about 50 mg of the samples were titrated in Hydranal-Coulomat AG reagent. Hyper differential scanning calorimetry (Diamond series DSC, Perkin-Elmer Ltd, USA) was used to measure $\Delta_{fus}H$ and T_m ($n=3$). Approximately 2.5 mg of sample was placed inside an aluminum pan which was subsequently sealed hermetically. The sample was subject to heating rates of 10 and 50°C/min under nitrogen purge rate of 20 ml/min. Thermogravimetric analysis (Universal, TA Instruments, USA) was performed on milled and crystallized adipic acid to analyze the weight loss with temperature. Approximately 25 mg of sample was used in each run with a ramp rate of 10°C/min. The X-ray diffraction patterns of crystallized and milled adipic acid were measured with an X-ray powder diffractometer (D8 Advance, Bruker AXS, GmbH, Germany). Measurements were performed with CuK$_\alpha$ radiation over the range of 5 to 50° (2θ) with steps of 0.04° ($t=1$ s/step). Powder diffraction data were verified by comparing to the standard reported in the Cambridge Structural Database.

RESULTS

From SEM images in Fig. 1, after milling, individual hexagonal-shaped adipic acid crystals were broken down into finer particles of less than 10 μm, which form agglomerates with size range similar to unmilled crystals. The DSC thermograms of crystallized and milled adipic acid measured at a heating rate of 10°C/min are presented in Fig. 2. After milling, the $\Delta_{fus}H$ of adipic acid was increased by 9% from 232.9 to 253.8 J/g. The onset T_m and peak T_m also increased from 148.40°C to 153.11°C and 152.38°C to 155.58°C, respectively. The higher values measured are consistent with previous reports on the DSC analyses of ground adipic acid (19).

To evaluate the role of electrostatic attractive forces on the change in melting properties, charge measurements were conducted using a Faraday cage connected to an electrometer. The average electrostatic charge density of milled adipic acid at 1.32×10^{-9} C/g was found to be slightly lower than that of crystallized particles at 1.52×10^{-9} C/g. It became apparent that with no increase in electrostatic charges after milling, it was unlikely that the increase in T_m and $\Delta_{fus}H$ was due to higher inter-particle electrostatic forces, which was

previously postulated. To calculate the additional energy needed to overcome the electrostatic charges between a primary particle and milled agglomerate, the electrostatic attractive force (27) was estimated using Eq. 1,

$$F_{ec} = \frac{\pi \times \sigma_1 \times \sigma_2}{4 \times \varepsilon_o} \times D_p^2 \qquad (1)$$

where F_{ec} is the electrostatic attractive force between two particles of diameter D_p, σ_1 and σ_2 are surface charge densities of the two particles and ε_o is the dielectric constant of vacuum. The additional energy contribution was estimated by multiplying this force with the inter-particle distance. Particle size of milled agglomerates was taken to be 600 μm (d_{40} from our past measurements) (11) and the particle size of primary particle to be approx. 6 μm (Fig. 1). As shown in Table I, the additional energy barrier (33.5×10^{-14} J/g) due to electrostatic attraction is insignificant with an order of magnitude 10^{14} times less than the measured increase in $\Delta_{fus}H$ (20.9 J/g). Therefore, the role of electrostatic forces in changing the melting properties of adipic acid was excluded.

The effect of particle size on $\Delta_{fus}H$ was studied by comparing DSC thermograms of sieved (250–500 μm) and unsieved both before and after milling. The results in Table II illustrated that a narrower size fraction did not result in any significant changes in $\Delta_{fus}H$ (0.1% to 1.1%) of milled and crystallized adipic acid, which was previously suggested.

To investigate the possible effect of thermal annealing of amorphous content during DSC measurements of $\Delta_{fus}H$, DSC analyses of crystallized and milled adipic acid were carried out at heating rates of 10 and 50°C/min. The results shown in Table II indicated that the different heating rates did not lead to significant differences in $\Delta_{fus}H$. For the crystallized adipic acid, only a small difference of 1.4% in the $\Delta_{fus}H$ was observed when different heating rates (10 and 50°C/min) were used. Similarly, a mere 0.55% difference in $\Delta_{fus}H$ was observed when the same ramp rates were used. This is in contrast to 13% to 16% difference reported on succinic acid using the same heating rates (14). To further examine the thermal annealing effect, the samples were heated or "annealed" at 120°C in DSC for 2 h, cooled to room temperature before the same DSC analyses were repeated. The thermograms prior and after heat treatment once again did not differ significantly (data not shown).
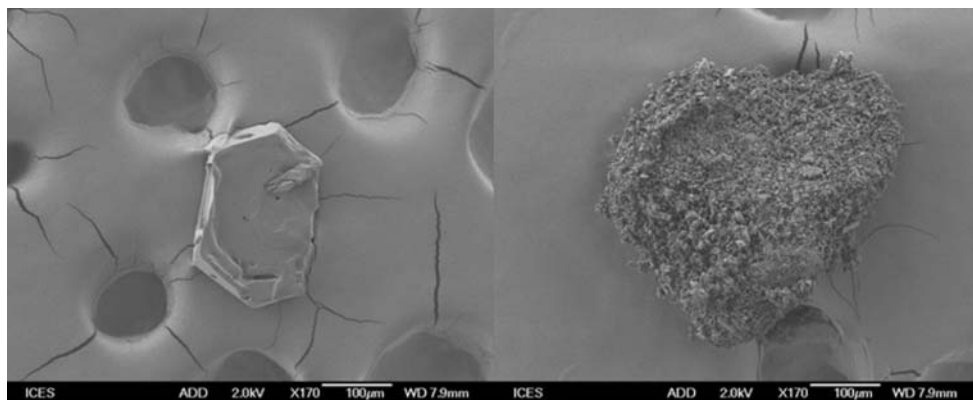

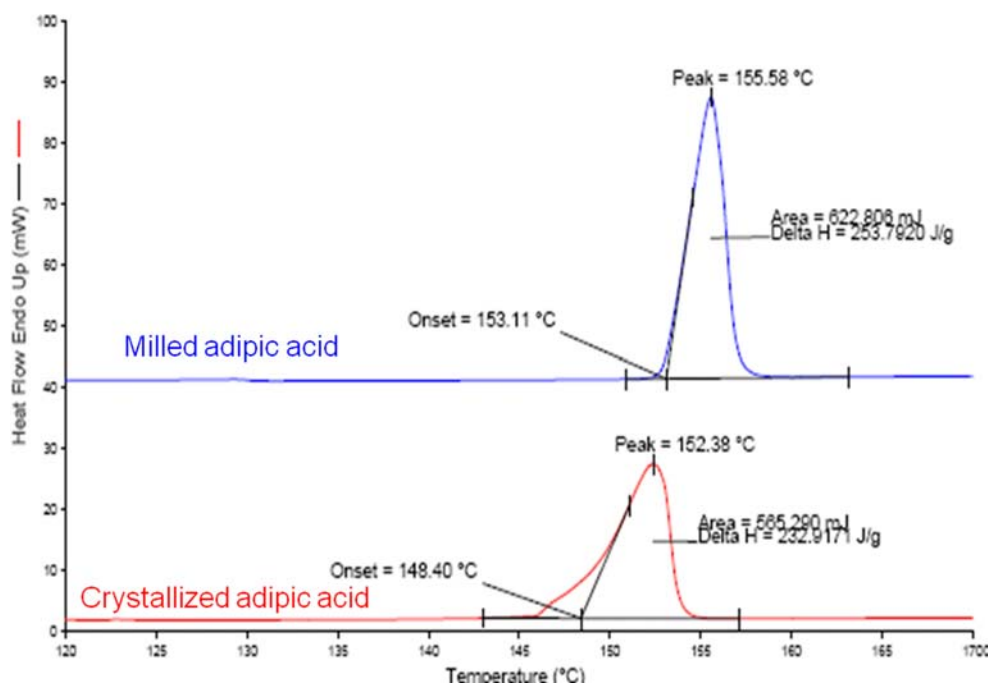**Fig. 1.** SEM images of crystallized adipic acid (*left*) and milled adipic acid (*right*)

Fig. 2. DSC thermograms of crystallized and milled adipic acid at a heating rate of 10°C/min

The absence of a thermal annealing effect could be explained by the low degree of amorphization of adipic acid during milling. As shown in Fig. 3, the PXRD diffractograms of crystallized and milled adipic acid indicated a largely crystalline material. The authors agree with Van Dooren and Müller (19) that if amorphous content were present, re-crystallization of the amorphous content via thermal annealing during DSC analysis, which is typically an exothermic process, should have theoretically lowered the $\Delta_{fus}H$ of milled adipic acid rather than the observed increase. This argument is in agreement with the melting point depression of milled Al due to a change in the microstructure as reported by Révész (9).

From Karl Fischer titration, the water content of crystallized adipic acid at 0.6 wt.% was six times higher than that of milled adipic acid at 0.1 wt.%. This tallied with the TGA thermograms in Fig. 4 showing a greater weight loss at 0.65% in crystallized adipic acid than at 0.11% in milled adipic acid when heated between 50°C and 150°C.

If water is regarded as an impurity in adipic acid, the change of T_m due to the mole fraction of water in crystallized adipic acid can be predicted using Eq. 2,

$$T_m = T_o - \frac{T_o^2 \times R \times X_i}{F \times \Delta H_f} \qquad (2)$$

where T_m is the melting temperature, T_o is the melting point of pure adipic acid (151.5–153°C), R is gas constant (8.314 J/(K mol)), X_i is the mole fraction of water, F is fraction of solid melted and ΔH_f is the enthalpy of fusion of pure adipic acid (2.385×10^5 J/kg) (28,29). After converting the values to SI units and taking $F=0.5$ as peak median in DSC thermogram, the melting point of crystallized adipic acid with impurity at 0.6 wt.% is shifted by 4°C to 148°C, which coincided with the measured onset T_m as shown in Fig. 2. In comparison, the much lower water content (0.11 wt.%) in milled adipic acid translates to a smaller depression of 0.6°C. The measured onset T_m is close to the calculated value and coincides with the reported value. Lin *et al.* (30) presented a solid–liquid phase diagram of adipic acid–water, which supports the melting point depression with increasing water content.

In order to examine the effect of water contents on $\Delta_{fus}H$ and T_m, while concurrently eliminating the influences of contaminants or impurities imparted during milling and milling-induced amorphization, crystallized adipic acid was

Table II. Effects of Particle Size Differences and Thermal Annealing of Amorphous Content on $\Delta_{fus}H$

Sample	$\Delta_{fus}H$ (J/g)	Difference in $\Delta_{fus}H$ (%)
Particle size uniformity		
Unsieved (crystallized)	246.2	1.1
Sieved (crystallized)	243.5	
Unsieved (milled)	259.0	0.1
Sieved (milled)	259.2	
Thermal annealing of amorphous content		
Crystallized adipic acid (@10°C/min)	235.5	1.4
Crystallized adipic acid (@50°C/min)	238.9	
Milled adipic acid (@10°C/min)	252.8	0.55
Milled adipic acid (@50°C/min)	254.2	

Table I. Effects of Electrostatic Charging on $\Delta_{fus}H$

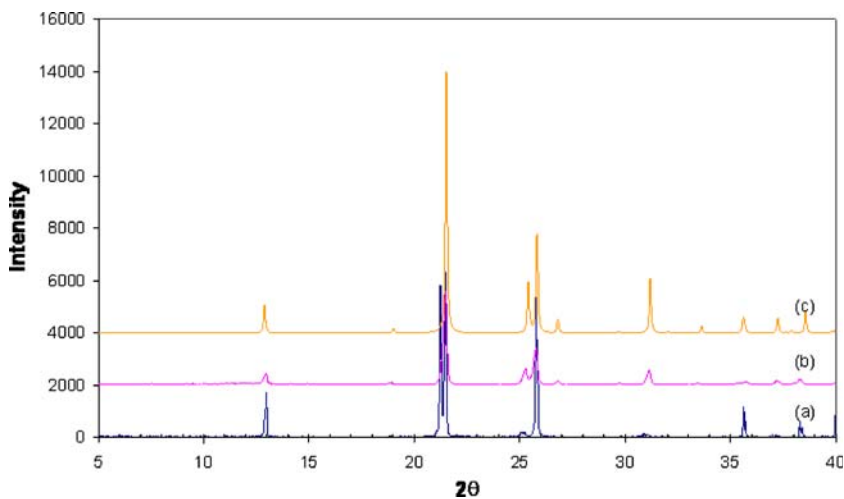| Milled sample	Additional energy required ($\times 10^{-13}$ J/g)
Electrostatic charging	
Primary	331.9
Agglomerate	3.3
Total	335.2

Fig. 3. Powder X-ray diffractograms of (*a*) crystallized, (*b*) milled adipic acid, and (*c*) reference from Cambridge database
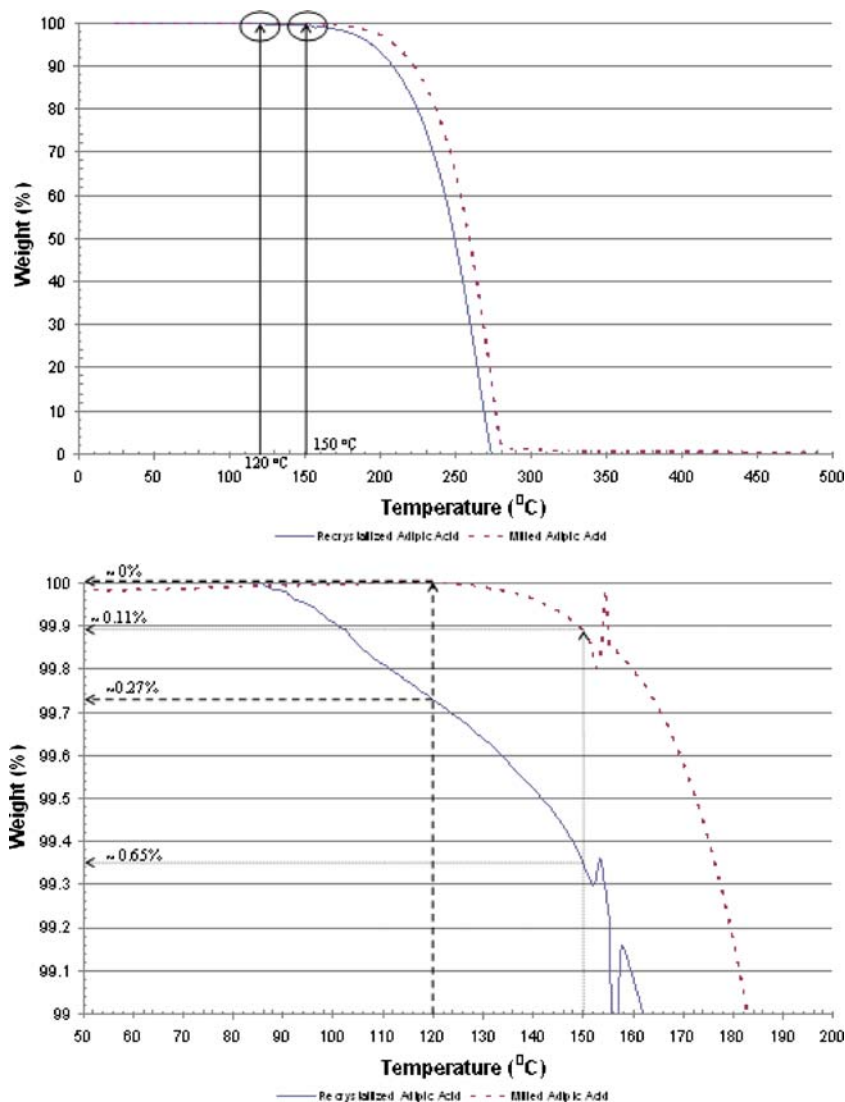

Fig. 4. TGA thermogram (*top*) of crystallized and milled adipic acid and enlarged view (*bottom*) at 120°C and 150°C

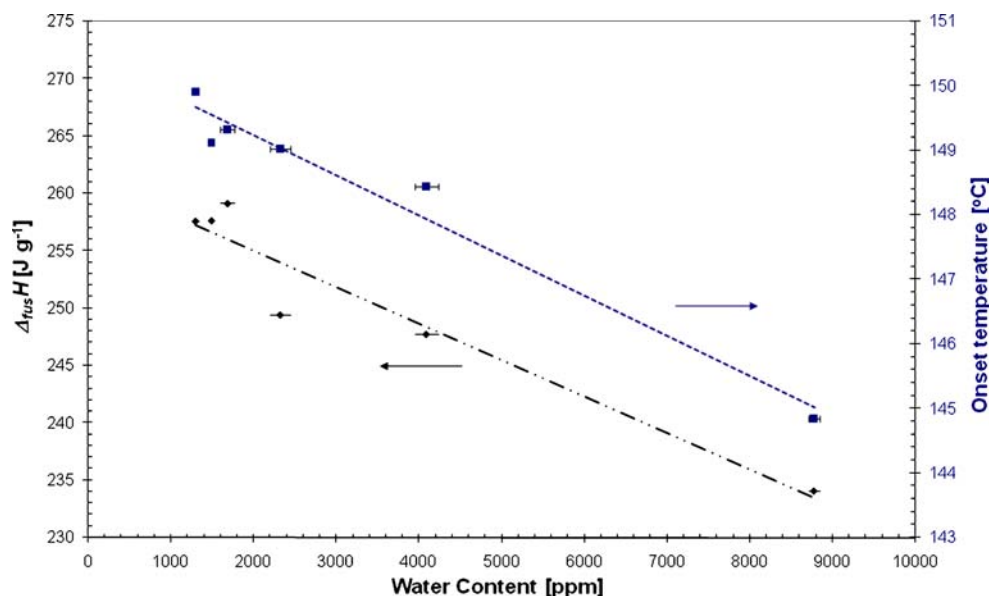**Fig. 5.** Plot of $\Delta_{fus}H$, and T_m against water content of crystallized adipic acid dried at 110°C over various durations

oven-dried at 110°C to vary the water content. Samples were taken at different time intervals from 0 to 8 h and analyzed using DSC. Figure 5 shows a plot of $\Delta_{fus}H$ and T_m against water content. The results revealed that a decrease in water content was accompanied by an increase in $\Delta_{fus}H$ and T_m, which show a clear correlation between water content in crystallized adipic acid and the melting properties.

However, such heat treatment of adipic acid has been reported to induce surface re-crystallization as shown under SEM (11). To eliminate the effects of heating and changes in surface morphology on melting properties, solution crystallization using different cooling rates was used to prepare adipic acid with different water contents. These samples were analyzed using DSC and the melting properties were plotted against the corresponding water content in Fig. 6. Like the oven-dried samples, the data clearly demonstrates the effect of water content on changing the $\Delta_{fus}H$ and T_m of adipic acid.

Water is likely to have been incorporated into the host adipic acid crystals during crystallization from solution (31). The water loss after milling can be explained by evaporation due to localized heating at newly cleaved surfaces during milling. Due to high mechanical and thermal stresses, the average milling temperature in a bench-top ball mill can rise by as much as 125°C to 180°C (21,32). Water freed from the adipic acid surfaces could have readily vaporized inside the milling jar. In fact, grinding in a mortar with a pestle for 5 min followed by drying has been reported as a method to remove included water inside adipic acid crystals (33).

The water content in particles can be broadly categorized into weakly and strongly bound. Weakly bound water includes adhesion, pore, occluded, and adsorbed water. Strongly bound water consists of lattice, inclusion, and constituent water (34). To understand the nature of water present in adipic acid, DSC analyses using two different
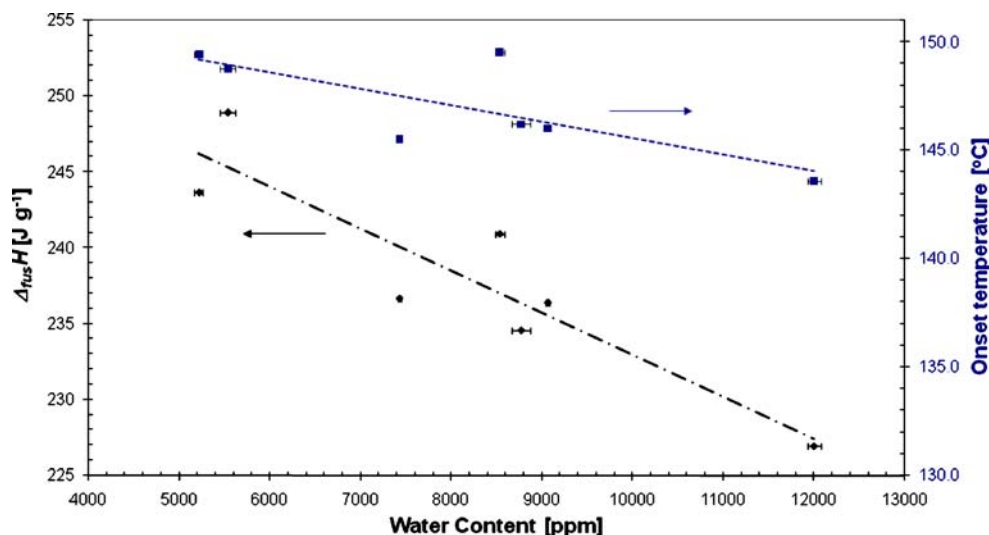

Fig. 6. Plot of $\Delta_{fus}H$ and T_m against water content of adipic acid obtained by crystallization at different cooling rates
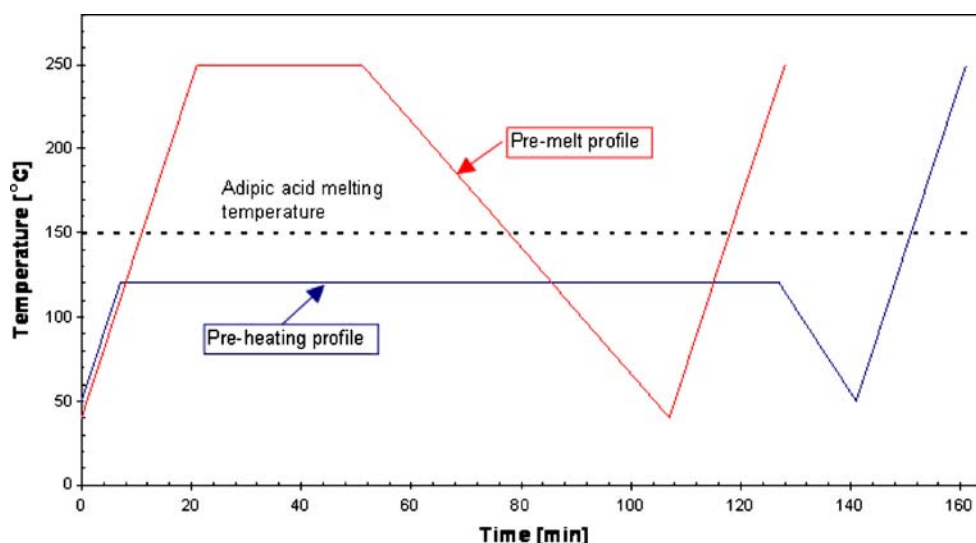
Fig. 7. DSC heating profiles

heating profiles were conducted as shown in Fig. 7. By heating the sample at 120°C for 120 min before measuring the melting properties, weakly bound water is removed. From Table III, the difference in $\Delta_{fus}H$ between crystallized and milled adipic acid was reduced from 9% to 7.5%, which still remained significant.

Earlier TGA results (Fig. 4) also showed that water was only partially removed at 120°C with weight losses of 0.27 and 0% for crystallized and milled adipic acid respectively. In an attempt to expel the strongly bound water, the samples were heated beyond the melting temperature (35), held at 250°C for 30 min to facilitate the removal of all bound water, and then solidified by cooling to room temperature before $\Delta_{fus}H$ was measured. As shown in Table III, the difference in $\Delta_{fus}H$ between crystallized and milled adipic acid was further reduced to 1.2%. Results suggest that water that plays a role in decreasing the $\Delta_{fus}H$ is predominantly strongly bound in adipic acid. The lower enthalpy of fusion of pre-melted adipic acid is due to evaporation of adipic acid during the isothermal step at 250°C for 30 min. As some adipic acid vapor has escaped from the DSC pan, the sample loss resulted in a lower $\Delta_{fus}H$ measured. Two endothermic events were reported in the TGA/DTA curve of adipic acid (34). The first was due to melting in the temperature range of 145°C to 189°C while the second was due to evaporation of adipic acid in the temperature range of 189°C to 301°C. Although adipic acid has no known stochiometric hydrate, the presence of

included water has been reported (22). Pre-heating at 120°C for 120 min may not be sufficient to remove most of the included water as normal drying processes are known to be inefficient in removing such liquid inclusions (33,36).

DISCUSSION

With the knowledge of the effect of liquid inclusions on the measured melting properties, a possible explanation is suggested to account for the differences between crystallized and milled adipic acid. As pockets of liquid water are dispersed inside crystallized adipic acid, the heating phase during DSC analysis would raise the solubility of adipic acid and cause it to dissolve into the water pockets. From 50°C to 100°C, the solubility of adipic acid increases significantly from 10 to 200 g/100 g of water (29). The adipic acid–water phase diagram shows that the SLE liquidus is continuous across all mole fractions. As both components are completely miscible at temperatures close to T_m, a concentrated adipic acid solution can be obtained at thermodynamic equilibrium (30). From TGA data, 0.27 wt.% of water is lost when temperature reaches at 120°C. As no DSC peaks were detected until this temperature, the latent heat of vaporization of water could be offset by the exothermic heat of solution when adipic acid gradually dissolves in water (29,37). As the temperature approaches T_m, pockets of saturated adipic acid solution are likely to vaporize very quickly. Below the reported T_m (151.5–153°C), at approximately 145°C, the start of a gradual endothermic peak was observed (Fig. 2). Upon further heating, the remaining pure adipic acid in the solid phase melts into the adipic acid solution, the melting endotherm emerges to overlap the vaporization event, which results in a skewed peak. As some of the adipic acid is already dissolved in the liquid state prior the onset of melting endotherm, the summation of events in the melting of remaining adipic acid in the solid-state, dissolution of adipic acid in water and vaporization of water results in a lower endotherm peak when compared to milled adipic acid. In milled adipic acid, the removal of water reduces the amount of adipic acid dissolved in water prior to melting and lowers

Table III. $\Delta_{fus}H$ of Milled and Crystallized Adipic Acid after Pre-heating and Pre-melt treatments

Sample	$\Delta_{fus}H$ (J/g)	Difference (%)
After pre-heating		
Milled	258.3	7.5
Crystallized	240.2	
After pre-melt		
Milled	213.5	1.2
Crystallized	210.9	

the quantity of exothermic heat of solution evolved. This results in a higher $\Delta_{fus}H$ measured as there is more adipic acid to be melted and less exothermic heat of solution available to compensate the endothermic vaporization of water.

CONCLUSIONS

The experimental study showed that the anomalous increase in $\Delta_{fus}H$ and T_m of adipic acid after milling was attributed to the loss of included water. As milling induces high mechanical and thermal stresses on crystallized adipic acid, the included water is partially removed due to localized hot spots on the particle surfaces. Previously postulated mechanisms such as triboelectrification, particle size uniformity and amorphous content did not explain the significant increase. By varying the water content in adipic acid in drying and crystallization experiments, the measured $\Delta_{fus}H$ and T_m values were found to be related to the water content. The removal of water in crystallized adipic acid by a pre-melt treatment prior DSC analysis also increased the $\Delta_{fus}H$ value close to that of milled adipic acid. The post-milling depression in T_m agreed with theoretical calculation based on the reduction in impurity (water) content. The higher $\Delta_{fus}H$ value of milled adipic acid could be due to the combined effect of dissolution of adipic acid in water inclusions, vaporization of water and melting of remaining adipic acid in the solid phase during DSC analysis.

ACKNOWLEDGMENTS

REFERENCES

1. Lee RW, Shaw JM, McShane J, Wood RW. Particle size reduction. In: Liu R, editor. Water-insoluble drug formulation. Denver: Interpharm; 2000. p. 455–88.
2. Stracey J, Tracy R. Secondary pharmaceutical production. In: Bennett B, Cole G, editors. Pharmaceutical production: an engineering guide. Rugby: IChem E; 2003. p. 111–201.
3. Rekhi GS, Sidwell R. Sizing of granulation. In: Parikh DM, editor. Handbook of pharmaceutical granulation technology. 3rd ed. Boca Raton: CRC, Taylor & Francis; 2005. p. 491–512.
4. Price R, Young PM. On the physical transformations of processed pharmaceutical solids. Micron. 2005;36:519–24.
5. Carstensen JT. Drugs and the pharmaceutical sciences vol. 110: advanced pharmaceutical solids. New York: Marcel Dekker; 2001. p. 323.
6. Zhang GZ, Gu C, Zell MT, Burkhardt RT, Munson EJ, Grant DJ. Crystallization and transitions of sulfamerazine polymorphs. J Pharm Sci. 2002;91:1089–100.
7. Thanatuksorn P, Kawai K, Kajiwara K, Suzuki T. Effects of ball-milling on the glass transition of wheat flour constituents. J Sci Food Agric. 2009;89:430–5.
8. Willart JF, Descamps M. Solid state amorphization of pharmaceuticals. Mol Pharmacol. 2008;5:905–20.
9. Révész Á. Melting behavior and origin of strain in ball-milled nanocrystalline Al powders. J Mater Sci. 2005;40:1643–6.
10. Berbenni V, Marini G, Bruni G, Maggioni A, Cogliati P. Thermoanalytical and spectroscopic characterization of solid state dipyridamole. J Therm Anal Calorim. 2002;68:413–22.
11. Ng WK, Kwek JW, Tan RB. Anomalous particle size shift during post-milling storage. Pharm Res. 2008;25:1175–85.
12. Joshi V, Dwivedi S, Ward GH. Increase in the specific surface area of budesonide during storage postmicronization. Pharm Res. 2002;19:7–12.
13. Vitez IM, Newman AW. Thermal microscopy. In: Duncan QMC, Reading M, editors. Thermal analysis of pharmaceuticals. Boca Raton: CRC, Taylor & Francis; 2007. p. 221–64.
14. Chikhalia V, Forbes RT, Storey RA, Ticehurst M. The effect of crystal morphology and mill type on milling induced crystal disorder. Eur J Pharm Sci. 2006;27:19–26.
15. Van Dooren AA, Müller BW. Influence of experimental variables on curves in differential scanning calorimetry. Part I. Study design and results of calibration checks. Thermochim Acta. 1981;49:151–61.
16. Van Dooren AA, Müller BW. Influence of experimental variables on curves in differential scanning calorimetry. Part II. Effects on baseline-related characteristics. Thermochim Acta. 1981;49:163–73.
17. Van Dooren AA, Müller BW. Influence of experimental variables on curves in differential scanning calorimetry. Part III. Effects on peak height, peak width, shape index and baseline displacement. Thermochim Acta. 1981;49:175–83.
18. Van Dooren AA, Müller BW. Influence of experimental variables on curves in differential scanning calorimetry. Part IV. Effects on peak-related temperatures and specific enthalpy. Thermochim Acta. 1981;49:185–91.
19. Van Dooren AA, Müller BW. Effects of heating rate and particle size on temperatures and specific enthalpies in quantitative differential scanning calorimetry. Thermochim Acta. 1982;54:115–29.
20. Steele G. Preformulation as an aid to product design in early drug development. In: Gibson M, editor. Pharmaceutical preformulation and formulation: a practical guide from candidate drug selection to commercial dosage form. Englewood: Interpharm; 2001. p. 175–289.
21. Feng T, Pinal R, Caravajal MT. Process induced disorder in crystalline materials: differentiating defective crystals from the amorphous form of griseofulvin. J Pharm Sci. 2008;97:3207–21.
22. Law D. Influence of composition of the crystallization medium on the physical properties and mechanical behavior of adipic acid crystals. PhD [dissertation]. University of Minnesota;1994.
23. Steele G. Predictions from small amounts of compound as an aid to candidate drug selection. In: Gibson M, editor. Pharmaceutical preformulation and formulation: a practical guide from candidate drug selection to commercial dosage form. Englewood: Interpharm; 2001. p. 21–96.
24. Dollimore D. Thermal analysis: differential calorimetry and differential thermal analysis. In: Meyers RA, editor. MEYERS: encyclopedia of analytical chemistry: applications, theory and instrumentation. West Sussex: Wiley; 2000. p. 13147–79.
25. Hojjati H, Rohani S. Measurement and prediction of solubility of paracetamol in water-isopropanol solution. Part 2: prediction. Org Process Res Dev. 2006;10:1110–18.
26. Keel TR, Thomson C, Davis MC, Tendler SJB, Roberts CJ. AFM studies of the crystallization and habit modification of an excipient material, adipic acid. Int J Pharm. 2004;280:185–98.
27. Masuda H, Gotoh K. Adhesive force of a single particle. In: Gotoh K, Masuda H, Higashitani K, editors. Powder technology handbook. New York: Marcel Dekker; 1997. p. 133–42.
28. Byrn S, Pfeiffer RR, Stowell JG. Solid-state chemistry of drugs. 2nd ed. SSCI, Inc.; 1999. p. 84–85.
29. Adi-pure®: high purity adipic acid [Internet]. INVISTA; c2005 [cited 2006 Jun 21]. Available from: http://adi-pure.invista.com/e-trolley/page_11546/index.html.
30. Lin HM, Tien HY, Hone YT, Lee MJ. Solubility of selected dibasic carboxylic acids in water, in ionic liquid of [Bmin][BF$_4$], and in aqueous [Bmin][BF$_4$] solutions. Fluid Phase Equilib. 2007;253:130–6.
31. Zhang GZZ, Grant DJW. Incorporation mechanism of guest molecules in crystals: solid solution or inclusion? Int J Pharm. 1999;181:61–70.

32. Ren R, Yang Z, Shaw LL. Polymorphic transformation and powder characteristics of TiO_2 during high energy milling. J Mater Sci. 2000;35:6015–26.

33. Zhang GZ, Grant DJ. Formation of liquid inclusions in adipic acid crystals during recrystallization from aqueous solutions. Cryst Growth Des. 2005;5:319–24.

34. Kawamura M. Moisture. In: Gotoh K, Masuda H, Higashitani K, editors. Powder technology handbook. New York: Marcel Dekker; 1997. p. 265–8.

35. Wright SF, Dollimore D, Dunn JG, Alexander K. Determination of the vapor pressure curves of adipic acid and triethanolamine using thermogravimetric analysis. Thermochim Acta. 2004;421:25–30.

36. Denbigh KG, White ET. Studies on liquid inclusions in crystals. Chem Eng Sci. 1966;21:739–54.

37. Musser MT. Adipic acid. In: Wiley-VCH, editor. Ullmann's encyclopedia of industrial chemistry. Weinheim: Verlag. KGaA; 2005. doi: 10.1002/14356007.a1_269.